

THE 20 AND 6 CENTIMETER RADIO LIGHT CURVES FOR SN 1981K: A TYPE II RADIO SUPERNOVA

SCHUYLER D. VAN DYK¹ AND KURT W. WEILER

Center for Advanced Space Sensing, Naval Research Laboratory, Code 4215, Washington, DC 20375-5000

RICHARD A. SRAMEK

National Radio Astronomy Observatory, P.O. Box O, Socorro, NM 87801

AND

NINO PANAGIA^{2,3}

Space Telescope Science Institute, 3700 San Martin Drive, Baltimore, MD 21218

Received 1991 December 23; accepted 1992 March 9

ABSTRACT

We present new observations of the radio supernova SN 1981K made with the VLA at 20 and 6 cm from 1985 March through 1990 May, augmenting previous observations which began in 1982 January and extended through 1984 November. Since the radio emission from supernovae appears to fall into distinct classes, we can establish after the fact an optical classification for SN 1981K solely from the radio data. From its 20 and 6 cm radio light curves, we conclude that SN 1981K was a Type II supernova, with radio properties similar to those of SN 1979C and SN 1980K.

Subject headings: radio continuum: stars — supernovae: individual (SN 1981K)

1. INTRODUCTION

Recent work has established the long-term behavior of the radio emission from two Type II supernovae (SNs): SN 1979C (Weiler et al. 1986, 1991) and SN 1980K (Weiler et al. 1986, 1992). Comparison of the observable properties derived from the radio light curves for these two SNs with the properties of other radio supernovae (RSNs) has also shown that the two objects form a distinguishable class of Type II RSNs (Van Dyk et al. 1992). Here we discuss another RSN, SN 1981K ($\alpha[1950.0] = 12^{\text{h}}16^{\text{m}}31^{\text{s}}23 \pm 0^{\text{s}}01$; $\delta[1950.0] = +47^{\circ}36'08''3 \pm 0''.2$), in NGC 4258, monitored now for nearly a decade, which appears to be a third member of this class of RSNs.

SN 1981K was discovered in 1982 January as an unresolved radio source on a 20 cm continuum map made by van der Hulst et al. (1983) using the Very Large Array (VLA).⁴ This source had not been previously detected to a limit of less than 0.25 mJy at 20 cm. Subsequent observations made using the Westerbork Synthesis Radio Telescope (WSRT) and the VLA indicated that the source was nonthermal and decreasing in flux density with time. It was suggested by van der Hulst et al. (1983) that the radio emission was from an unidentified supernova which probably occurred between 1981 May and 1982 January (cf. Weiler et al. 1986), a suggestion which was confirmed by Wild (1983; see also van der Hulst et al. 1983), who found that optical images from 1981 August showed a transient object near the SN position.

Weiler et al. (1986) presented the available measurements of SN 1981K at wavelengths 20 and 6 cm through 1984 Novem-

ber. We present here new radio results from 1985 through 1990 May. These more complete light curves define the evolution of radio emission from SN 1981K over more than 8 yr and indicate that this supernova is quite similar to SN 1979C and SN 1980K in its radio properties and is therefore likely to be a member of the same class of Type II RSNs (cf. Van Dyk et al. 1992).

2. OBSERVATIONS

The new observations of SN 1981K were made with the VLA at 20 cm (1.490 GHz) and 6 cm (4.860 GHz) from 1985 March through 1990 May at a quarterly rate. Since monitoring of an evolving radio source requires measurement at frequent intervals, we were not able to request specific VLA configurations and consequently have measurements at all array sizes. Along with each observation of the source, a short observation of a "secondary," possibly variable, calibrator, 1216+487, was made at each frequency. To establish an absolute flux density scale, most observing sessions also included an observation of a "primary," presumed constant, calibrator, 3C 286.

At long wavelengths and short VLA baselines (i.e., low resolving power), the high flux density per beam area from the disk emission of NGC 4258 confuses the radio emission from SN 1981K. Therefore, measurement of SN 1981K at 20 cm in C- and D-configurations and, at later times when the radio emission had considerably weakened, at 6 cm in D-configuration, was not possible. Only (3 σ) upper limits to the flux densities for SN 1981K could be estimated at those epochs.

Since SN 1981K has now weakened to the point that further monitoring at 20 and 6 cm is very difficult and time-consuming, even with the VLA, and since additional data points with poor signal-to-noise ratio are unlikely to greatly add to our knowledge of the radio properties of SN 1981K (see §§ 4.1 and 4.3), these new measurements, along with those made by Weiler et al. (1986), represent the complete set of monitoring data for this RSN.

¹ Naval Research Lab/National Research Council Cooperative Research Associate.

² Affiliated with the Astrophysics Division, Space Science Department of ESA.

³ Also University of Catania, Italy.

⁴ The VLA is operated by the National Radio Astronomy Observatory of Associated Universities, Inc., under a cooperative agreement with the National Science Foundation.

TABLE 1
CALIBRATION SOURCES

Source Name (1)	Calibrator Type (2)	$\alpha_{1950.0}$ (3)	$\delta_{1950.0}$ (4)	S_{20} (Jy) (5)	S_6 (Jy) (6)	S_2 (Jy) (7)
3C 286	Primary	Not used	Not used	14.45	7.42	3.45
1216+487 ^a	Secondary	12 ^h 16 ^m 38 ^s .570	+48°46'34"90			

^a See Table 2 for flux densities.

2.1. Calibration

The VLA is described in a number of publications (e.g., Thompson et al. 1980; Hjellming & Bignell 1982; Napier, Thompson, & Ekers 1983); the general procedures for RSN observations, with analysis of the possible sources of error, are discussed in Weiler et al. (1986). The "primary" calibrator employed here, 3C 286, was assumed to be constant in flux density with time and to have the flux densities at 20 and 6 cm given in Table 1.

The "secondary" calibrator, 1216+487, was used as the phase (position) and amplitude (flux density) reference for the observations of SN 1981K. Its assumed position (epoch 1950.0) is given in Table 1, and its flux density values, measured against 3C 286 or assumed based on values at other observing epochs, at 20 cm (S_{20}) and 6 cm (S_6) are presented for each observing epoch in Table 2.

2.2. Data Reduction

After the data were initially calibrated using standard soft-

TABLE 2
MEASURED OR ASSUMED FLUX DENSITY VALUES FOR
THE SECONDARY CALIBRATOR 1216+487

Observation Date (1)	S_{20} (Jy) (2)	S_6 (Jy) (3)	S_2 (Jy) (4)
1985 Mar 30	0.887 ^a	0.719 ^a	...
1985 Jun 29	0.943 ^a	0.794 ^a	...
1985 Aug 22	0.970 ^a	0.826 ^a	...
1985 Dec 14	0.923 ^a	0.791 ^a	...
1986 Mar 28	0.850 ^b	0.680 ^c	...
1986 Jun 16	0.850 ^b	0.680 ^c	...
1986 Sep 25	0.803 ^a	0.647 ^a	...
1986 Dec 15	0.800 ^d	0.680 ^c	...
1987 Mar 5	0.680 ^a	...
1987 Jun 24	0.800 ^d	0.680 ^c	...
1987 Sep 18	0.669 ^a	...
1987 Dec 20	0.673 ^a	...
1988 Mar 31	0.673 ^c	...
1988 Sep 16	0.759 ^a	0.654 ^a	0.770 ^a
1988 Dec 29	0.654 ^a	0.658 ^a	0.747 ^a
1989 Apr 6	0.670 ^a	0.650 ^a	...
1989 Jul 17	0.689 ^a	0.693 ^a	...
1989 Dec 21	0.672 ^a	...
1990 Feb 12	0.711 ^a	...
1990 May 29	0.683 ^a	0.625 ^a	...

^a Independently calibrated using 3C 286.

^b Not independently calibrated. Calibration values at 20 cm taken as an approximate average of the values measured on 1985 December 14 and 1986 September 25.

^c Not independently calibrated. Calibration values at 6 cm adopted from 1987 March 5.

^d Not independently calibrated. Calibration values at 20 cm adopted from 1986 September 25.

^e Not independently calibrated. Calibration value at 20 cm adopted from 1987 December 20.

ware packages on the DEC-10 and Convex computers at the VLA, the data were "exported" to the Naval Research Lab for analysis with AIPS on the local VAX 11/785 and Alliant VFX/40 computers. Most data sets were individually hand-edited, mapped, CLEANed, inspected, and measured independently in both IF channels for each observing band. The values from the two IF channels were then averaged to obtain a final measurement of the flux density in each band at each epoch. Observations after 1989 April were mapped by combining both IF channels into a single map before measurement.

2.3. Errors

One estimate for the flux density measurement error is the rms "map" error which measures the contribution of small, unresolved fluctuations in the background emission and random map fluctuations due to receiver noise. For strong sources this can be considered only a lower limit to the total error. Comparison of the two IF channel flux density solutions also provides an error estimate but is clearly too small a sample to provide meaningful statistics; also, the two IF channels do not provide truly independent solutions for a number of types of instrumental errors. Therefore, errors for the measurements in this paper include a basic 5% error to account for the normal inaccuracy of VLA flux density measurements and any absolute scale error for the primary calibrator, 3C 286. The final errors, σ_f , listed in Table 3, are taken as

$$\sigma_f^2 \equiv (0.05S_0)^2 + \sigma_0^2, \quad (1)$$

where S_0 is the observed flux density for SN 1981K and σ_0 is the observed rms map error measured outside of any obvious regions of emission.

3. RESULTS

Since the previous publication of SN 1981K data in Weiler et al. (1986), we have added 11 new measurements (and four upper limits) at 20 cm and 18 new measurements (and one upper limit) at 6 cm. We present these results in Table 3. Column (1) is the date of observation; column (2) is the time in days since the estimated date of optical maximum of 1981 August 15 (the date of explosion is taken by Weiler et al. 1986 to have been ~ 15 days before optical maximum, or ~ 1981 July 31); column (3) gives the VLA configuration in which the supernova was observed; columns (4) and (6) give the measured flux densities at 20 cm (S_{20}) and 6 cm (S_6), respectively; and columns (5) and (7) give the error estimates for these measurements. Table 3 also contains determinations of spectral index, α , from our data ($S \propto \nu^{+\alpha}$), with column (8) listing the spectral index, α_6^{20} , between 20 and 6 cm, and column (9), its error, $\sigma_{\alpha_6^{20}}$.

In Figure 1 we plot the time evolution of the flux density of SN 1981K at 20 and 6 cm, including both the new results and the results for earlier epochs from Weiler et al. (1986). The solid

TABLE 3
NEW FLUX DENSITY AND SPECTRAL INDEX MEASUREMENTS FOR SN 1981K^{a,b}

OBSERVATION DATE (1)	TIME SINCE OPTICAL MAXIMUM ^c (days) (2)	VLA CONFIGURATION (3)	FLUX DENSITY				SPECTRAL INDEX ($S \propto \nu^{+\alpha}$)	
			S_{20} (mJy) (4)	σ_{20} (mJy) (5)	S_6 (mJy) (6)	σ_6 (mJy) (7)	α_6^{20} (8)	$\sigma_{\alpha_6^{20}}$ (9)
1981 Aug 15	$\equiv 0$							
1985 Mar 30	1323	A/B	1.10	0.15	0.41	0.08	-0.83	0.21
1985 Jun 28	1413	B/C	1.23	0.27	0.48	0.12	-0.80	0.28
1985 Aug 9	1455	VLA	1.30 ^d	0.12
1985 Aug 22	1468	C	<1.33 ^e	...	0.59	0.10
1985 Dec 14	1582	D	<4.80 ^e	...	0.39	0.14
1986 Mar 28	1686	A	1.28	0.11	0.39	0.07	-1.01	0.17
1986 Jun 16	1766	A/B	1.21	0.24	0.50	0.11	-0.75	0.25
1986 Sep 25	1867	B/C	1.44	0.34	0.69	0.09	-0.62	0.23
1986 Dec 15	1948	C	1.21	0.48	0.40	0.13	-0.94	0.44
1987 Mar 5	2028	D	0.30	0.10
1987 Jun 24	2139	A	1.18	0.12	0.52	0.10	-0.69	0.19
1987 Sep 18	2225	A	0.57	0.07
1987 Dec 20	2318	B	0.67	0.06
1988 Mar 31	2420	C	0.63	0.08
1988 Sep 16	2589	D	<2.46 ^e	...	0.33	0.13
1988 Dec 29	2693	A	0.67	0.11	0.30	0.06	-0.80	0.22
1989 Apr 6	2791	B	0.70	0.15	0.42	0.07	-0.49	0.24
1989 Jul 17	2893	C	<1.16 ^e	...	0.39	0.08
1989 Dec 21	3050	D	<0.27 ^e
1990 Feb 12	3103	D/A	0.33	0.06
1990 May 29	3209	A	0.69	0.10	0.41	0.05	-0.44	0.16

^a For previous measurements, cf. Weiler et al. 1986.

^b Measurements at 2 cm on 1988 September 16 and 1988 December 29 produced only 3 σ upper limits of <0.60 mJy and <0.69 mJy, respectively.

^c Although having little effect on the model fit (see text), the date of explosion is taken to be 1981 July 31, 15 days before the assumed date of optical maximum of 1981 August 15 (cf. Weiler et al. 1986).

^d Hummel & Krause 1987.

^e 3 σ upper limit.

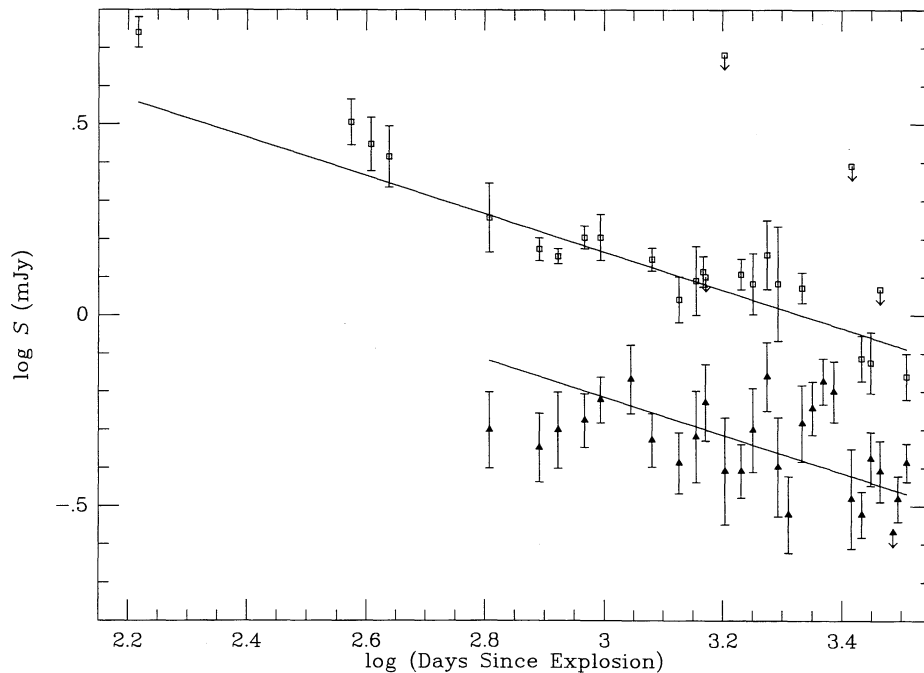


FIG. 1.—Radio “light curves” for SN 1981K in NGC 4258. The two wavelengths, 20 cm (*open squares*) and 6 cm (*filled triangles*), are shown together. The data represent more than 8 yr of observations for this object, including new observations presented in this paper and previous measurements from Weiler et al. (1986). The age of the supernova is measured in days from the estimated date of explosion of 1981 July 31 (15 days before the approximate date of optical maximum of 1981 August 15). The solid lines represent the best-fit light curves of the form $S(\text{mJy}) = K_1[\nu/(5 \text{ GHz})]^2[t - t_0/(1 \text{ day})]^2$, with the assumption that the absorption of the radio emission at 20 and 6 cm has been negligible ($\tau \sim 0$) over the duration of the observations.

lines are the “best-fit” model light curves discussed below. In Figure 2 we show the change in spectral index between 20 and 6 cm with time over the near decade since explosion. One can see from Table 3 and Figure 2 that the spectral index values are very similar to those found by Weiler et al. (1986), with α_6^{20} continuing to scatter about a value of ~ -0.8 , indicating that the gas has been optically thin to emission at these two wavelengths since radio discovery. The solid curve shown in Figure 2 is not an independent fit, but is calculated from the model light curves shown in Figure 1. We made two measurements at 2 cm on 1988 September 16 and 1988 December 29, but they yielded only 3σ upper limits of less than 0.60 mJy and less than 0.69 mJy, respectively.

4. DISCUSSION

4.1. Radio Light Curves

Previous studies of RSNs (see, e.g., Weiler et al. 1986; Weiler & Sramek 1988; Weiler et al. 1991) have shown that the radio emission from most RSNs (with the exception of those resembling SN 1986J; cf. Weiler, Panagia, & Sramek 1990) can be described by the relation

$$S(\text{mJy}) = K_1 \left(\frac{\nu}{5 \text{ GHz}} \right)^\alpha \left(\frac{t - t_0}{1 \text{ day}} \right)^\beta e^{-\tau}, \quad (2)$$

with

$$\tau = K_2 \left(\frac{\nu}{5 \text{ GHz}} \right)^{-2.1} \left(\frac{t - t_0}{1 \text{ day}} \right)^\delta, \quad (3)$$

where S is the observed flux density at frequency ν on date t after explosion date t_0 . As previously, we assume that the radio emission is nonthermal with spectral index α and varies with age $t - t_0$ to the power β . Any optical depth τ present is due to

thermal, free-free absorption in an ionized medium ($\nu^{-2.1}$) external to the radio-emitting region with a radial dependence $\rho \propto r^{-2}$ from a red supergiant progenitor wind of constant speed. Accepting the Chevalier (1981a, b; 1984a, b) model fixes the optical depth time-dependence power δ as

$$\delta \equiv \alpha - \beta - 3. \quad (4)$$

K_1 and K_2 are scaling parameters for the units of choice and formally correspond to the flux density and optical depth, respectively, at 5 GHz 1 day after explosion.

Since Figure 2 does not show the steepening of spectral index with time expected from optical depth effects (see, e.g., Weiler et al. 1986), we conclude that the 20 and 6 cm emission from SN 1981K has been optically thin since first detection and take $\tau \equiv 0$.

The full available data set at 20 and 6 cm, including the values from Weiler et al. (1986), was then used to solve for the three free parameters, K_1 , α , and β , in equation (2). The date of explosion, t_0 , is not well constrained by the data and, following Weiler et al. (1986), was defined to be 1981 July 31, 15 days before the approximate date of optical maximum of 1981 August 15. The “best” fit was obtained by using a minimum reduced χ^2 procedure to identify the best value and range of values for each of the parameters, and these are listed in Table 4. A minimum measurement error of 15% was needed to bring χ_{red}^2 down from ~ 2.5 to ~ 1.0 per degree of freedom. This need to increase the data errors beyond the level of $\sim 5\%$ for points taken near maximum flux density in order to obtain a $\chi_{\text{red}}^2 \sim 1$ implies, not unexpectedly, that the model of equation (2) is not sufficiently complex to describe the details of any short-term fluctuations in the light curves. The range of uncertainty listed for each parameter in Table 4 is the amount that the parameter must deviate from the best-fit value in order to increase χ_{red}^2 from ~ 1 to ~ 3.5 (Abramowitz & Stegun 1965). This is appro-

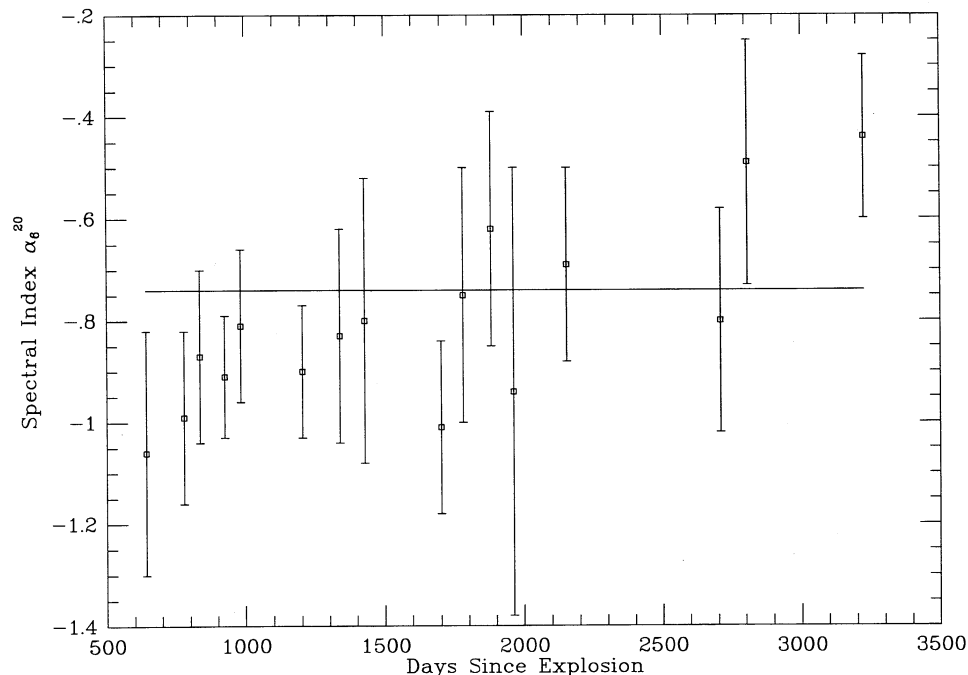


FIG. 2.—Spectral index α ($S \propto \nu^\alpha$) evolution for SN 1981K between 20 cm and 6 cm, plotted as a function of time, in days, since the assumed explosion date of 1981 July 31 (15 days before the estimated date of optical maximum of 1981 August 15). The solid line is calculated from the best-fit theoretical “light curves” shown in Fig. 1. The optical depth of any intervening matter has apparently been optically thin at both 20 and 6 cm since earliest radio detection.

TABLE 4
FITTING PARAMETERS FOR SN 1981K^a

Parameter (1)	Value (2)	Deviation Range ^b (3)
K_1	19	12–25
α	–0.74	–(0.18–1.06)
β	–0.50	–(0.46–0.56)
K_2	$< 1.5 \times 10^5$
$\delta (\equiv \alpha - \beta - 3)$	3.24	–(2.62–3.60)
t_0	\equiv 1981 July 31	1975 Jul 27–1982 Jan 13

^a The radio light curves are assumed to fit a curve of the form $S(\text{mJy}) = K_1 [v/5 \text{ GHz}]^\alpha [(t - t_0)/1 \text{ day}]^\beta$, where any optical depth τ has been negligible throughout the observing period.

^b The deviation range is the range in which there is a $\sim 67\%$ probability that the true value lies ($\chi^2_{\text{red}} \sim 3.5$ for a three parameter fit). This is equivalent to a 1σ range for a one parameter solution.

^c The date of the explosion is chosen to be 1981 July 31 (15 days before the approximate date of optical maximum of 1981 August 15), following Weiler et al 1986. The fit is not very sensitive to this choice.

appropriate for a three-parameter fit and determines the 67% probability intervals within which the true values lie; that is, the error range analogous to the 1σ uncertainty for a single-parameter fit. The model curves calculated by equation (2) for the parameter values of Table 4 are shown as the solid lines in Figure 1. The radio emission of SN 1981K is clearly declining in a regular manner, albeit with some small, short-term fluctuations about the general trend. In Figure 2 we can see that the spectral index is also very well behaved and well described by equation (2) with the parameters from Table 4.

With the much larger number of data points now available at both 20 and 6 cm, it is not unexpected that the values of the fitting parameters given in Table 4 significantly differ from those parameters ($K_1 = 73 \pm 6$; $\alpha = -0.91 \pm 0.07$; $\beta = -0.73 \pm 0.06$; $\delta \equiv \alpha - \beta - 3 = -3.18 \pm 0.09$) determined from the much more limited data set available to Weiler et al. (1986). In particular, the spectral index α is less steep, the rate of decline β is much flatter, and the 6 cm flux density on day 1, K_1 is significantly smaller. The deceleration parameter $m = -\delta/3 \equiv (\alpha - \beta - 3)/3$ (see Weiler et al. 1986) remains ~ 1 to within the errors.

Although it is impossible to explicitly determine from the existing data for SN 1981K the value of the initial optical

depth parameter K_2 in equation (3), it is possible to derive an upper limit. This is accomplished by assuming that the first flux density value at 20 cm (van der Hulst et al. 1983; Hummel et al. 1983; see also Weiler et al. 1986) is the peak observable flux density in this wavelength band and then increasing the value of K_2 in equations (2) and (3) until the model curve in Figure 1 at 20 cm reaches a “maximum” and “turns over” at this first data point. This upper limit to K_2 is also given in Table 4.

4.2. Models

Two models, the “minishell” and the “miniplerion,” have been suggested to provide the mechanism for acceleration of the relativistic particles generating the nonthermal emission for RSNs. However, for all presently known RSNs, only the minishell model has been found to be appropriate. Because its light curve behavior is so similar to a number of other known examples, we shall assume that this is also the case for SN 1981K.

4.3. The Type of SN 1981K

Van Dyk et al. (1992) show that RSNs fall into several distinct classes based on the observable radio properties of spectral index α , decline rate β , “turn-on” rate, peak luminosity, peak external absorption (K_2), and (if present) a peak internal absorption. In Table 5 we present these properties for SN 1981K along with the same properties for SN 1979C and SN 1980K. The data for SN 1979C are taken from Weiler et al. (1991); the data for SN 1980K are taken from Weiler et al. (1992). As discussed above, the turn-on for SN 1981K was not observed, so that only upper limits can be given for K_2 and the turn-on rate.

Examination of Table 5 shows a number of similarities among the three RSNs: (1) all three have relatively steep nonthermal spectral indices (α); (2) all three have relatively slow declines in radio flux density after maximum (β); and (3) all three have relatively rapid turn-on rates.

Some variation in these parameters among the objects is also clear, especially the relatively large differences in initial spectral luminosities and initial external absorptions. However, when compared with other known RSNs, such as Type Ia (not radio emitters; see, e.g., Weiler et al. 1986), Type Ib (very rapid radio turn-on and off; see, e.g., Weiler et al. 1986), and other Type II SNs such as SN 1986J (slow turn-on at each frequency and early detection at low frequencies; see

TABLE 5
OBSERVABLE RADIO PROPERTIES OF SN 1981K COMPARED WITH THOSE OF
SN 1979C AND SN 1980K

PROPERTY	SUPERNOVA		
	1981K	1979C ^a	1980K ^b
Spectral index (α)	–0.74	–0.74	–0.52
Decline rate after maximum (β)	–0.50	–0.78	–0.66
Turn-on rate ^c at 6 cm	< 4.3	0.5	2.1
Initial ($t - t_0 = 1$ day) spectral luminosity ^d at 6 cm [$K_1(4\pi d^2)$]	1.0×10^{27}	4.8×10^{29}	2.7×10^{27}
Initial ($t - t_0 = 1$ day) external absorption at 6 cm (K_2)	$< 1.5 \times 10^5$	3.6×10^7	3.4×10^5

^a Data from Weiler et al. 1991.

^b Data from Weiler et al. 1992.

^c Turn-on rate is defined as $dS_6(\text{norm})/dt$ at epoch $t - t_0$ when $S_6(\text{norm}) = 50$. $S_6(\text{norm}) = [S_6/S_6(\text{max})] \times 100$; units are d^{-1} .

^d Units of spectral luminosity are $\text{ergs s}^{-1} \text{Hz}^{-1}$; distances to parent galaxies ($d = 6.8$ Mpc for NGC 4258 [SN 1981K], $d = 16.8$ Mpc for NGC 4321 [SN 1979C], $d = 5.5$ Mpc for NGC 6946 [SN 1980K]) are from Tully 1988.

Weiler et al. 1990), SN 1981K clearly and quite closely resembles SN 1979C and SN 1980K. Although we reserve detailed discussion of classes of RSNs to another paper (Van Dyk et al. 1992), SN 1981K clearly represents a new member of the class resembling SN 1979C.

SN 1981K was not optically classified, but its radio properties strongly suggest that it was a Type II, similar to SN 1979C and SN 1980K. Thus, it appears possible that, at least in some cases, long-term monitoring of the radio emission from a SN can provide a means for determining optical classification even when the SN was not optically well observed. Also, the similarity in radio properties to SN 1979C and SN 1980K implies that SN 1981K arose from a red supergiant progenitor, as is thought to be the case for both SN 1979C and SN 1980K (see Weiler et al. 1986).

4.4. The Mass of the Stellar Progenitor

Although data showing the initial transition of the radio emission from SN 1981K from optically thick to optically thin are missing, which allow us to set only an upper limit to K_2 (see Table 4), it is interesting to place an upper limit on the mass loss rate for its assumed red supergiant progenitor star by using the simplified formula of equation (16) in Weiler et al. (1986). Adopting a wind velocity, $w \sim 10 \text{ km s}^{-1}$, an assumed optical expansion velocity of the supernova ejecta, $v_i \sim 1 \times 10^4 \text{ km s}^{-1}$, and an electron temperature in the wind similar to that applied to SN 1979C and SN 1980K (cf. Weiler et al. 1991, 1992), $T \sim 3 \times 10^4 \text{ K}$ (Lundqvist & Fransson 1988), the mass loss is then estimated to be $\dot{M} < 5 \times 10^{-6} M_\odot \text{ yr}^{-1}$. Assuming that the wind velocity, w , during this mass loss was constant, the duration of this mass loss epoch, Δt_M , is the ratio of the radius of the wind-blown circumstellar shell, R_{shell} , to the velocity w . From the known time ($\sim 8.5 \text{ yr}$) of interaction of the rapidly moving SN ejecta ($v_i \sim 10^4 \text{ km s}^{-1}$) with the shell material, which gives rise to the observed radio emission, we can estimate $R_{\text{shell}} \gtrsim 2.7 \times 10^{17} \text{ cm}$. If the shell was established by a red supergiant wind moving at $\sim 10 \text{ km s}^{-1}$, a duration of high mass loss of $\Delta t_M \gtrsim 8.5 \times 10^3 \text{ yr}$ must hold. Since the mass loss rate is determined by the red supergiant progenitor mass

(e.g., Maeder & Meynet 1988), and since SN 1981K has a lower estimated mass loss rate than either SN 1979C or SN 1980K (see Weiler et al. 1991, 1992), we conclude that SN 1981K originated from a less massive star. In fact, SN 1981K represents the least massive example of a Type II RSN we have so far encountered.

5. CONCLUSIONS

The new observations define a much better set of fitting parameters than was possible by Weiler et al. (1986) with their much more limited data set. Because it is now so faint, the observations presented here, along with the measurements made by Weiler et al., also represent the complete set of radio data likely to be obtained for SN 1981K. The following conclusions can be formed from study of this data set.

1. The radio emission from SN 1981K is continuing its regular decline in flux density with time.

2. The light curves, including the most recent data, are still consistent with the minishell model for nonthermal emission with purely external, thermal absorption.

3. The observable radio properties of SN 1981K are consistent with it being a member of a class of Type II RSNs similar to SN 1979C and SN 1980K.

4. The long-term monitoring of radio emission from SN 1981K provides a means for identifying its optical type as Type II, even though it was not optically well observed at the time of explosion.

5. An upper limit on the mass loss from the assumed red supergiant progenitor for SN 1981K can be established as less than $5 \times 10^{-6} M_\odot \text{ yr}^{-1}$ for $\gtrsim 10^4 \text{ yr}$ before explosion.

6. The upper limit to its mass-loss rate implies that the progenitor of SN 1981K was less massive than the progenitors of either SN 1979C or SN 1980K; it had, in fact, the least massive precursor star of any Type II RSN yet detected.

We wish to thank Jennifer L. Discenna for her assistance at the Naval Research Laboratory in the production and analysis of the radio maps of SN 1981K.

REFERENCES

- Abramowitz, M., & Stegun, I. A. 1965, *Handbook of Mathematical Functions* (New York: Dover) 980
- Chevalier, R. A. 1981a, *ApJ*, 246, 267
- . 1981b, *ApJ*, 251, 259
- . 1984a, in *Ann. NY Acad. Sci.* 422, 215
- . 1984b, *ApJ*, 285, L63
- Hjellming, R. M., & Bignell, R. C. 1982, *Science*, 216, 1279
- Hummel, E., & Krause, M. 1987, private communication
- Hummel, E., van der Hulst, J. M., Davies, R. D., Pedlar, A., & van Albada, G. D. 1983, *IAU Circ.*, No. 3803
- Lundqvist, P., & Fransson, C. 1988, *A&A*, 192, 221
- Maeder, A., & Meynet, G. 1988, *A&AS*, 76, 411
- Napier, P. J., Thompson, A. R., & Ekers, R. D. 1983, *Proc. IEEE*, 71, 1295
- Thompson, A. R., Clark, B. G., Wade, C. M., & Napier, P. J. 1980, *ApJS*, 44, 151
- Tully, R. B. 1988, *Nearby Galaxies Catalog* (Cambridge: Cambridge Univ. Press)
- van der Hulst, J. M., Hummel, F., Davies, R. D., Pedlar, A., & van Albada, G. D. 1983, *Nature*, 306, 566
- Van Dyk, S. D., Weiler, K. W., Panagia, N., & Sramek, R. A. 1992, in preparation
- Weiler, K. W., Panagia, N., & Sramek, R. A. 1990, *ApJ*, 364, 611
- Weiler, K. W., & Sramek, R. A. 1988, *ARA&A*, 26, 295
- Weiler, K. W., Sramek, R. A., Panagia, N., van der Hulst, J. M., & Salvati, M. 1986, *ApJ*, 301, 790
- Weiler, K. W., Van Dyk, S. D., Panagia, N., & Sramek, R. A. 1992, *ApJ*, in press
- Weiler, K. W., Van Dyk, S. D., Panagia, N., Sramek, R. A., & Discenna, J. L. 1991, *ApJ*, 380, 161
- Wild, P. 1983, *IAU Circ.*, No. 3803.